

Supporting Information

Application of Non-precious Bifunctional Catalysts for Metal-Air Batteries

Steffen Haller, Vladislav Gridin, Kathrin Hofmann, Robert W. Stark, Barbara Albert, Ulrike I. Kramm

Calculation of the H₂O₂ yield and the electron transfer number n_{app} was conducted based on the measured disc current j_{disc} and ring current j_{ring} using the following formula:^[1]

$$n = 100 \frac{4 j_{\text{ring}}}{j_{\text{disc}}} \quad (\text{S1})$$

and

$$\frac{j_{\text{ring}}}{j_{\text{disc}}} = \frac{N_{\text{ring}}}{4} \quad (\text{S2})$$

with the collection efficiency of the ring $N_{\text{ring}} = 0.38$.

From the obtained slopes m in the KL plots, n_{KL} was calculated by the following formula:^[2]

$$n_{\text{KL}} = \frac{m}{m_0} \quad (\text{S3})$$

with $F = 96485 \text{ C mol}^{-1}$, $D_0 = 1.9 \cdot 10^{-5} \text{ cm}^2 \text{ s}^{-1}$, $\nu = 0.01 \text{ cm}^2 \text{ s}^{-1}$ and $c_{\text{O}}^0 = 1.2 \cdot 10^{-6} \text{ mol cm}^{-3}$.

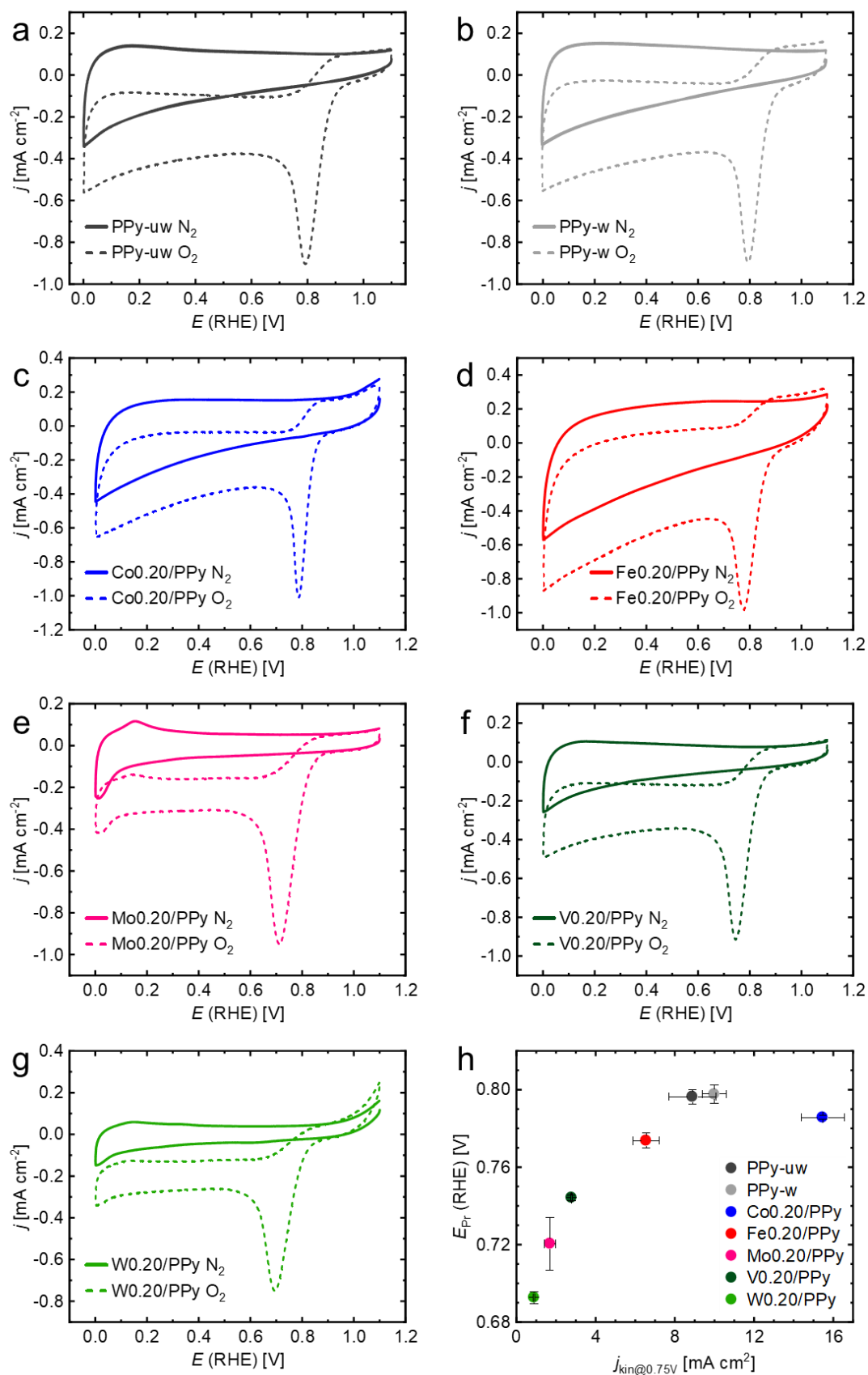


Figure S1: Cyclic voltammograms in N_2 - and O_2 -saturated electrolyte, recorded at scan rates of $10\ mV\ s^{-1}$: (a) PPy-uw, (b) PPy-w, (c) Co0.20/PPy, (d) Fe0.20/PPy, (e) Mo0.20/PPy, (f) V0.20/PPy, (g) W0.20/PPy, (h) peak reduction potentials E_{Pr} plotted against kinetic current densities at 0.75 V.

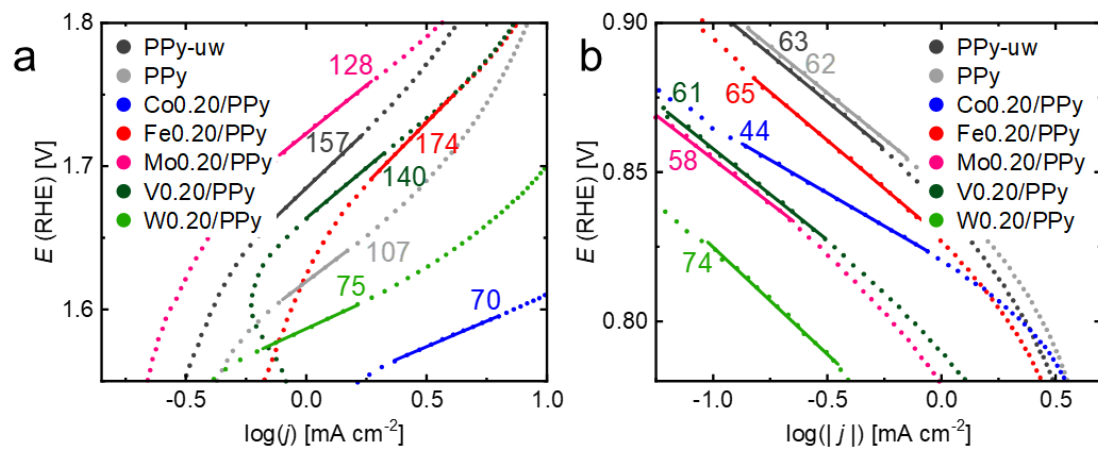


Figure S2: Transition metal variation series: (a) OER Tafel plots, (b) ORR Tafel plots, with Tafel slopes in mV dec^{-1} .

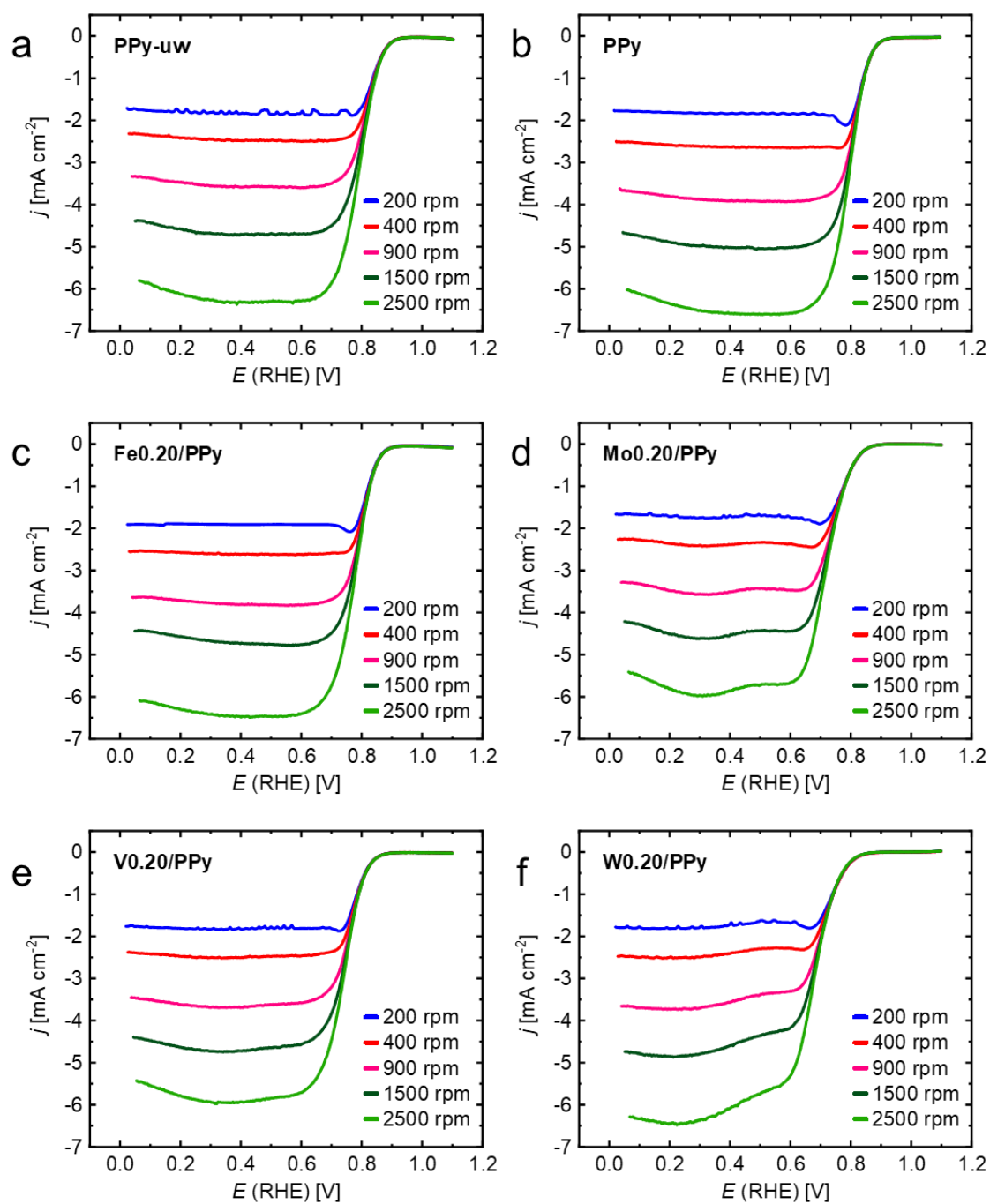


Figure S3: ORR curves recorded at 200, 400, 900, 1500 and 2500 rpm for (a) PPy-uw, (b) PPy, (c) Fe0.20/PPy, (d) Mo0.20/PPy, (e) V0.20/PPy, (f) W0.20/PPy.

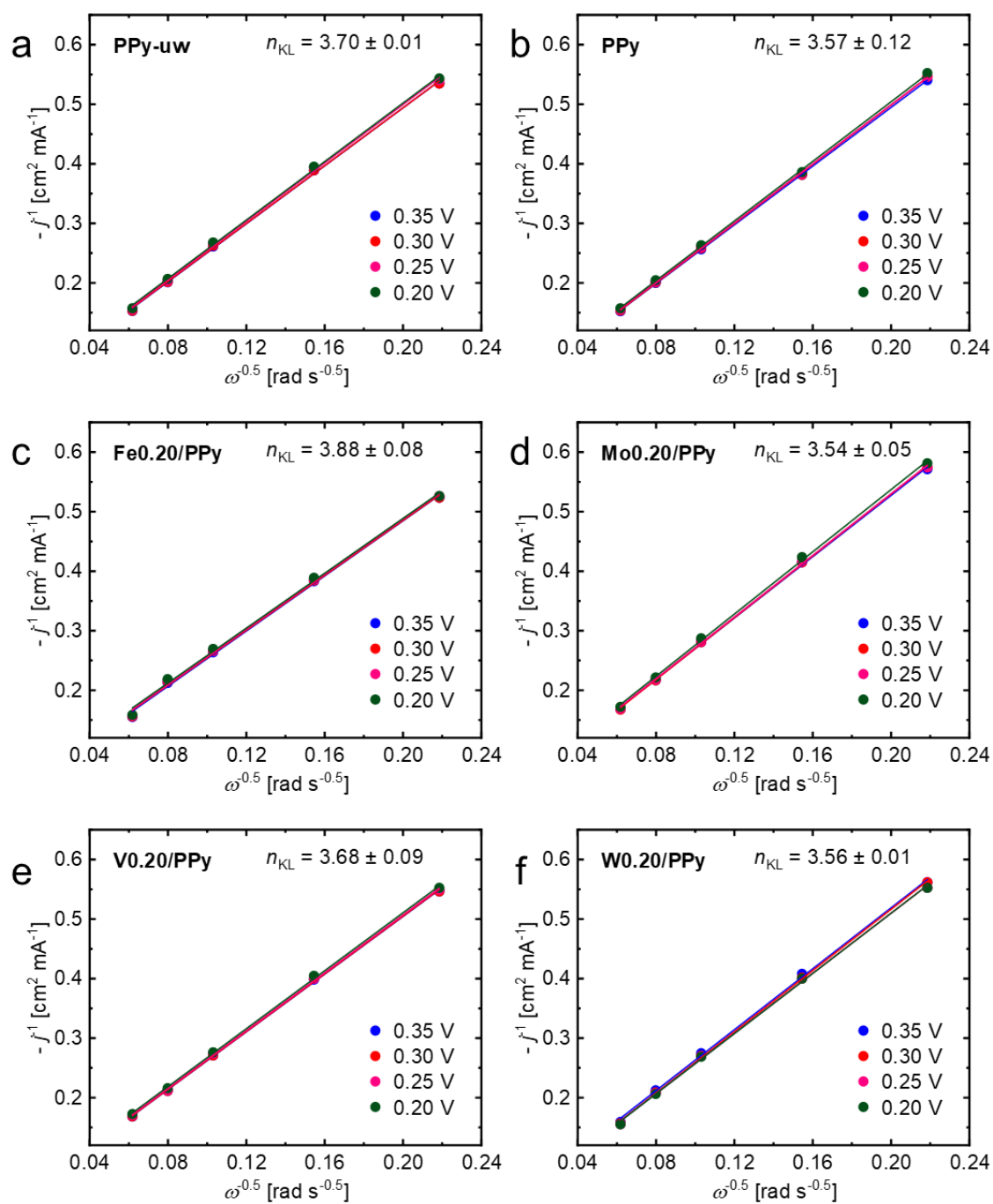


Figure S4: Koutecký-Levich plots of (a) PPy-uw, (b) PPy, (c) Fe0.20/PPy, (d) Mo0.20/PPy, (e) V0.20/PPy, (f) W0.20/PPy.

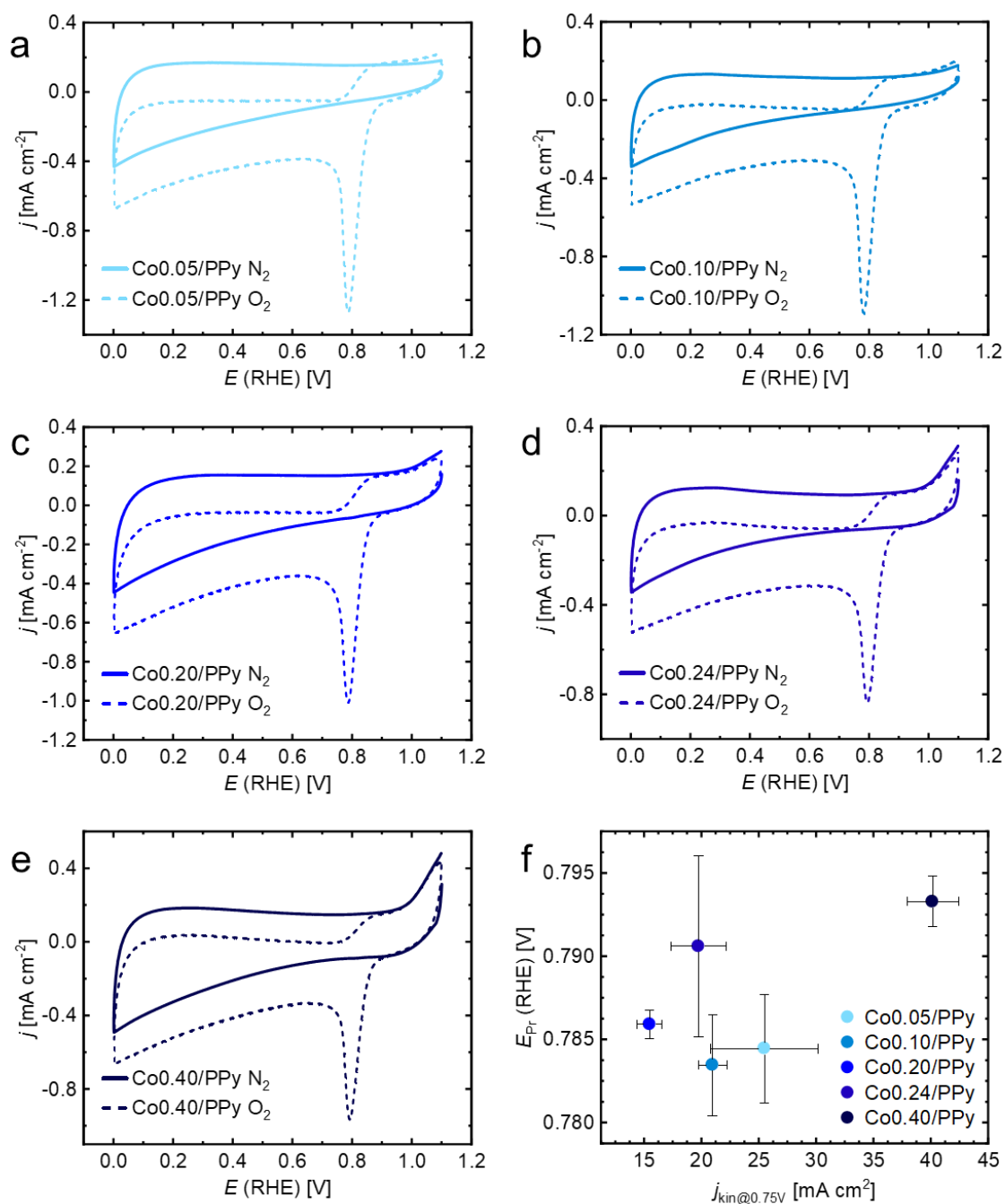


Figure S5: Cyclic voltammograms in N₂- and O₂-saturated electrolyte, recorded at scan rates of 10 mV s⁻¹: (a) Co0.05/PPy, (b) Co0.10/PPy, (c) Co0.20/PPy, (d) Co0.24/PPy, (e) Co0.40/PPy, (f) peak reduction potentials E_{Pr} plotted against kinetic current densities at 0.75 V.

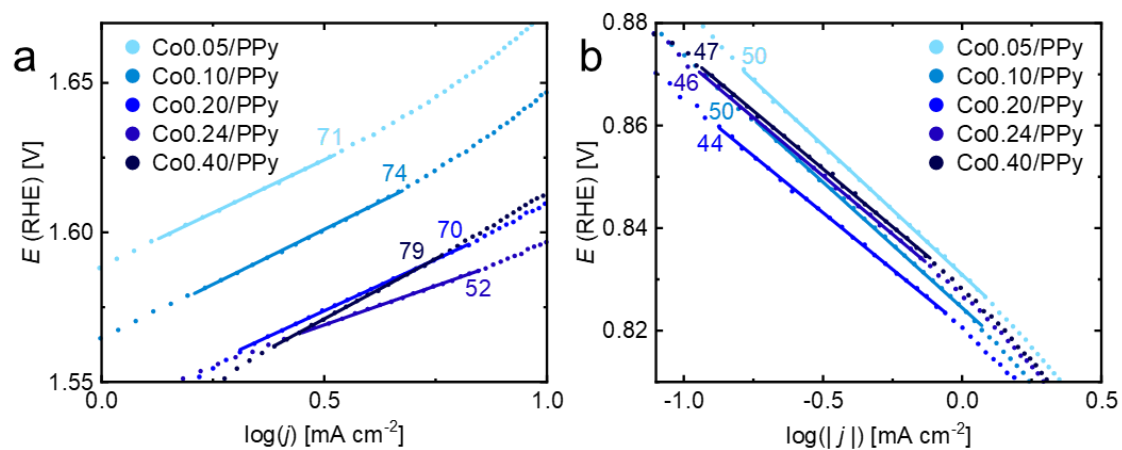


Figure S6: Cobalt loading variation series: (a) OER Tafel plots, (b) ORR Tafel plots, with Tafel slopes in mV dec^{-1} .

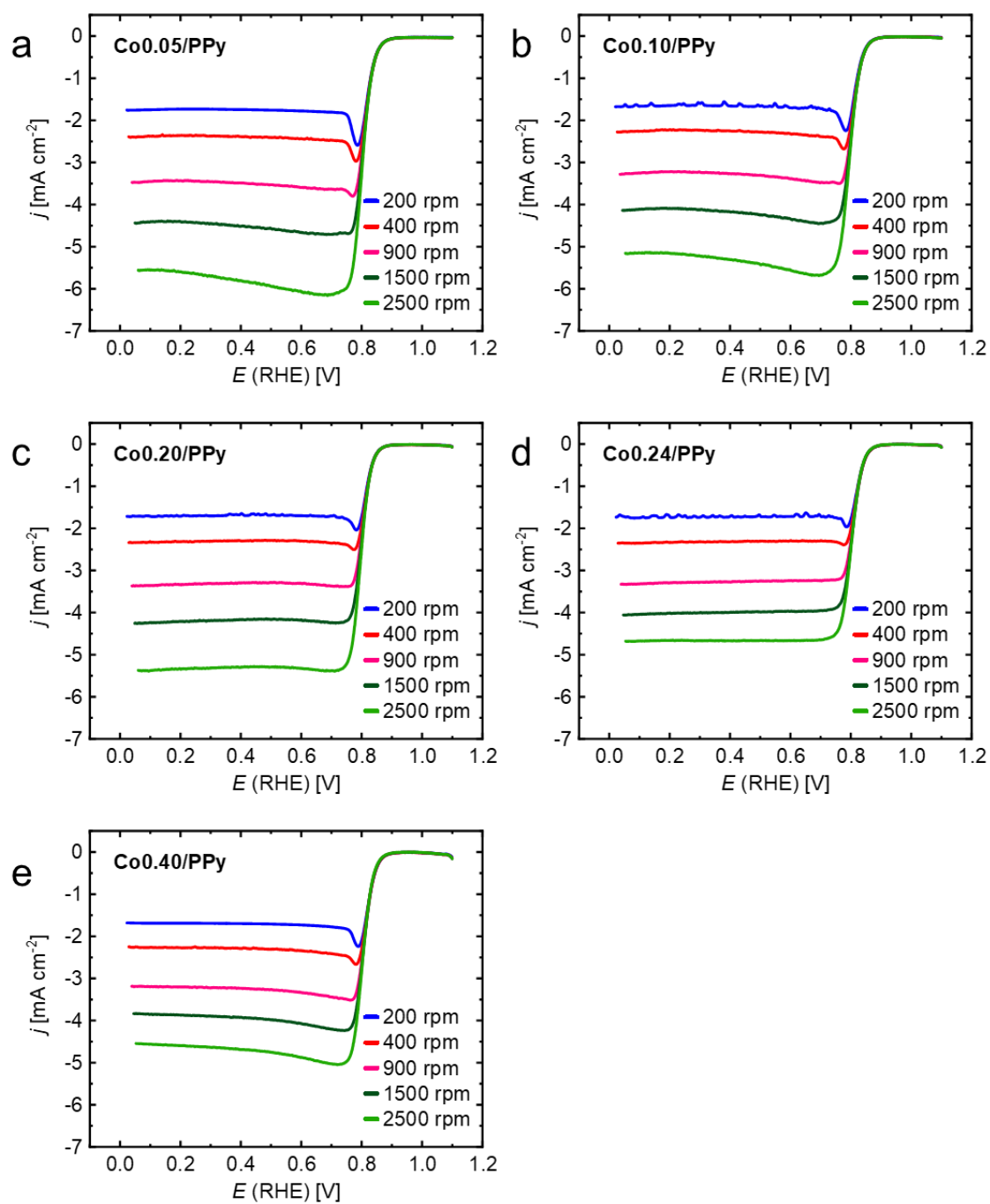


Figure S7: ORR curves recorded at 200, 400, 900, 1500 and 2500 rpm for (a) Co0.05/PPy, (b) Co0.10/PPy, (c) Co0.20/PPy, (d) Co0.24/PPy, (e) Co0.40/PPy.

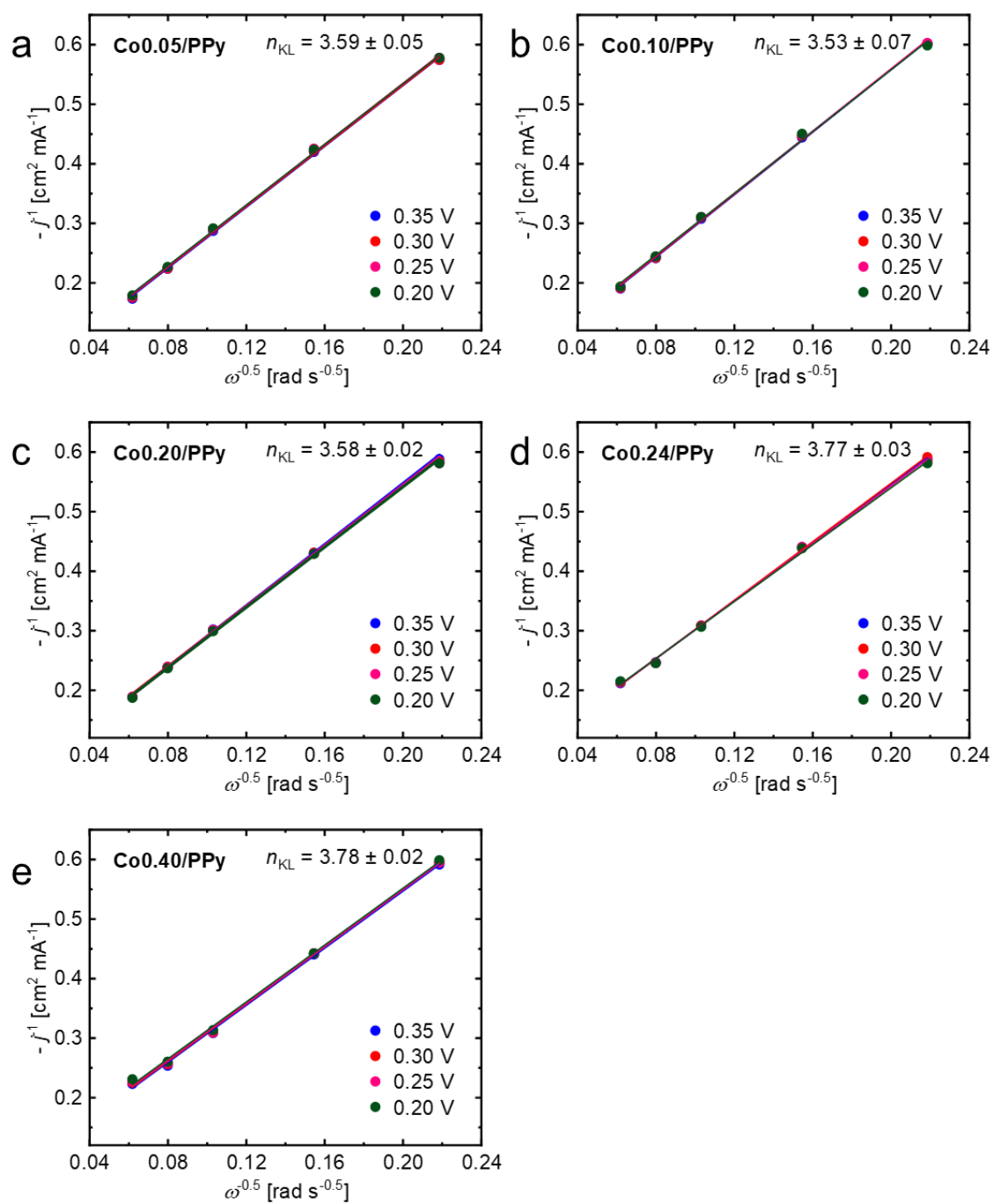


Figure S8: Koutecký-Levich plots for (a) Co0.05/PPy, (b) Co0.10/PPy, (c) Co0.20/PPy, (d) Co0.24/PPy, (e) Co0.40/PPy.

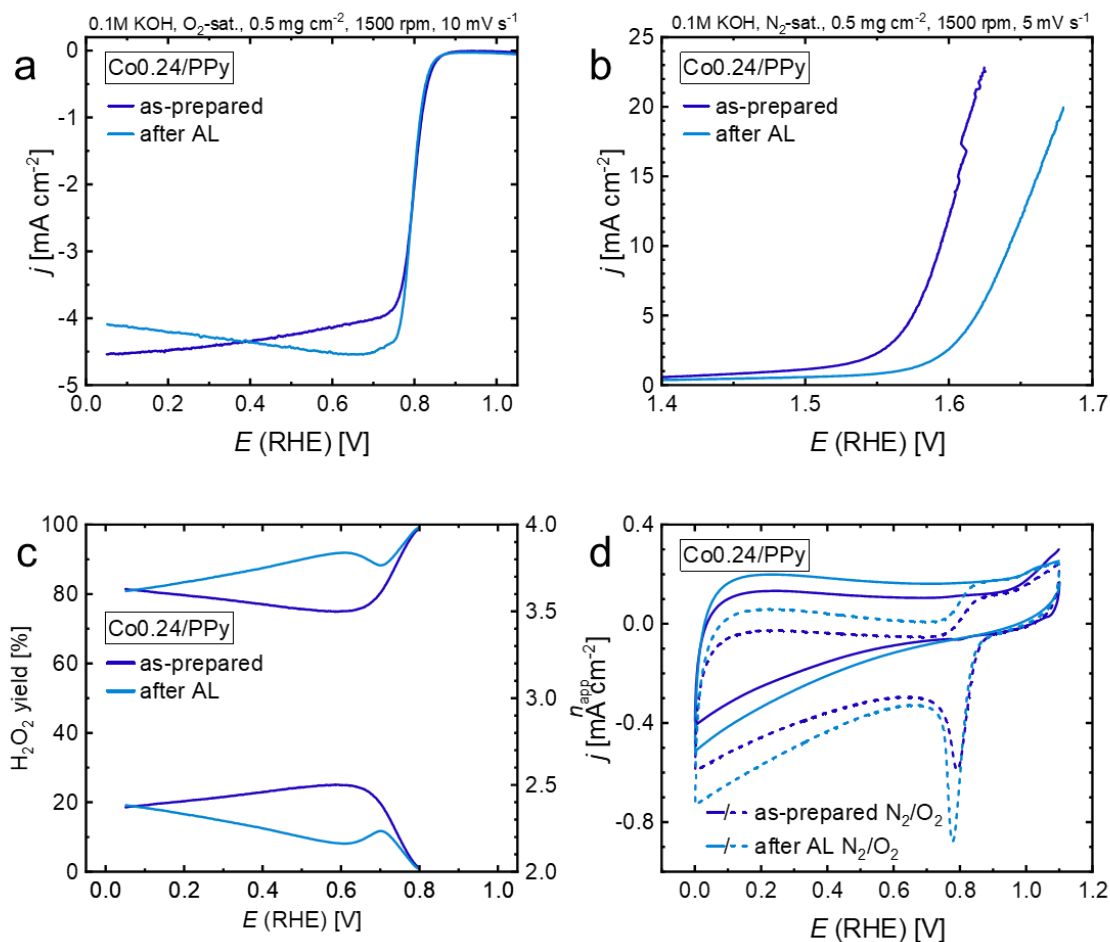


Figure S9: Acid-leaching (AL) of Co_{0.24}/PPy: (a) ORR curves, (b) OER curves, (c) peroxide yield and apparent electron transfer number, (d) CVs recorded in N₂- and O₂-saturated electrolyte. Please note that the catalyst displayed here was prepared from a different polypyrrole batch as well as a larger microwave pyrolysis batch.

- [1] Z. Jia, G. Yin, J. Zhang, *Rotating Ring-Disk Electrode Method*, in: *Rotating electrode methods and oxygen reduction electrocatalysts* (Eds: W. Xing, G. Yin, J. Zhang), Elsevier **2014**, 199 – 229.
- [2] C. Dua, Q. Tana, Yina. G, J. Jiujun Zhangb, *Rotating Disk Electrode Method*, in: *Rotating electrode methods and oxygen reduction electrocatalysts* (Eds: W. Xing, G. Yin, J. Zhang), Elsevier **2014**, 171 – 198.